EXPERIMENTAL VALIDATION OF AN ULTRAVIOLET IMAGING CUBE SATELLITE

Jason L. Grillo[1], Troy F. Hajjar[1], Brady E. Hill[1], Kodi A. Rider[2], Thomas J. Immel[2], Eltahry Elghandour[1]

[1]California Polytechnic State University

San Luis Obispo, CA

[2]Space Sciences Laboratory, University of California Berkeley

Berkeley, CA

ABSTRACT

Space based ultraviolet (UV) imaging has produced a number of critical results over the years for geospace science. There is a compelling scientific need for future NASA missions to make space-based observations from multiple vantage points and from one or more orbit planes. This highlights a need for UV imaging instruments that fit into small volumes, including CubeSats ranging from 3U to 12U in size. UC Berkeley (UCB) Space Sciences Laboratory (SSL) is developing a proposal to support this need using a constellation of eight 12U CubeSats.

The main research objective of this paper is the experimental validation of the instrument's front optics design. The instrument was evaluated for its image focus and boresight alignment before and after it was subjected to a series of launch environment tests specified by NASA's General Environmental Verification Standard (GEVS) [1]. Environmental tests were performed at California Polytechnic State University, San Luis Obispo, which consisted of several vibration tests and a thermal vacuum test. The image quality of the instrument outperformed the specifications defined by the design requirements by an order of magnitude. As such, the front optics assembly of the ultraviolet imaging cube satellite will survive the launch and space environment.

1. INTRODUCTION

1.1 Purpose

Space-based ultraviolet (UV) imaging has produced several critical results over the years for geo-space science (e.g. [4-7]). New UV observations implementing updated imaging technology can further advance a number of scientific objectives in space science. The research group from California Polytechnic State University, San Luis Obispo, worked in conjunction with the Space Sciences Laboratory (SSL) at the University of California, Berkeley, to design, manufacture, and test an ultra-violet imaging instrument for a CubeSat application. A compact FUV imager of this volume could be extensively deployed to geosynchronous orbits at low cost. The Cal Poly research team was tasked with providing a proof-of-concept for the front 1-unit, or 1U, of the satellite, where the optical assembly is housed. The optical assembly sits on a datum plate, and

Copyright 2019. Used by the Society of the Advancement of Material and Process Engineering with permission.

SAMPE Conference Proceedings. Charlotte, NC, May 20-23, 2019. Society for the Advancement of Material and Process Engineering – North America.

consists of a field stop, baffles that define the instrument field of view, and a lens mount and keeper subassembly that houses the glass lenses of the instrument. The instrument is presented in Figure 1. The interface between the optics assembly and structure is a multifunctional material interface with an embedded Viton elastomer layer to dampen higher order vibration frequencies and amplitudes [2].

Figure 1. The front 1U of the UV CubeSat instrument (left) and optics assembly (right).

A series of environmental tests were performed to validate the front optics assembly design to the set of requirements defined in Table 1. First, the instrument's image performance was assessed before subjecting the instrument to environmental conditions. Second, the instrument image performance was evaluated after thermal vacuum (TVAC) cycles. Third, the image performance was measured after random vibration excitation. Finally, the repeatability of the image performance measurements was determined to assess the validity of the conclusion. The image performance methods are described in Section 1.2, and the applicable environmental testing conditions are explained in Section 1.3. Overall, this described exploration is prepared for individuals involved in the aerospace industry concerned with environmental testing as a means of validating a design.

Table 1. Applicable instrument performance requirements defined by SSL.

Designator	Requirement
UVI-1-2	The UVI instrument shall have a 30° circular field of view (FOV).
UVI-1-4	The UVI boresight shall remain aligned to within 0.25° post launch with respect to its initial on-ground alignment.
UVI-1-5	The UVI spot sizes shall remain below 20 microns (TBR) post launch with respect to its initial on-ground alignment.
UVI-1-6	The variation in the relative angular orientation of the UVI boresight shall be maintained to within 0.25° under the thermal conditions expected on-orbit.
UVI-1-7	The variation in the spot sizes of the UVI boresight shall remain below 20 microns under the thermal conditions expected on-orbit.

1.2 Instrument Image Performance

The fundamental task of the design project is to maintain alignment of the optics hardware after the instrument undergoes the harsh environments of launch and orbit. A series of measurements were taken to verify the performance integrity of the instrument after experiencing vibration and thermal loads. Functionality was verified using Optical Ground Support Equipment (OGSE), which used a pinhole laser as the light source. The instrument interfaced to the baseplate of the OGSE in a repeatable and accurate manner, which is shown in Figure 2 below. The tests necessary to verify performance include field of view, boresight alignment, and average spot size. The details of each testing plan are presented in the sections below.

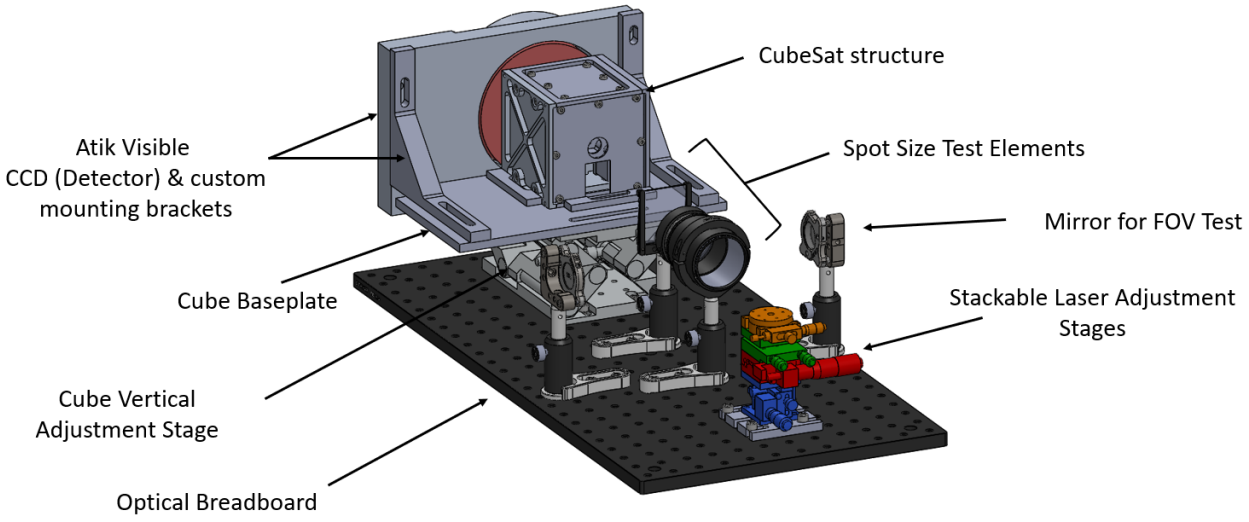

Figure 2. OGSE used to measure the instrument image performance.

1.2.1 Boresight Alignment Measurement

Perpendicularity of the instrument optics with respect to the laser light source was achieved by calibrating the laser rotary stages against the instrument fiducial cube. The laser was raised vertically until the beam was centered through the apertures. The spot centroid of the laser was recorded by counting the number of pixels from the top corner of the image to the centroid, as illustrated in Figure 3. Small changes in the relative position of the two lenses in the optics assembly were observed through this measurement.

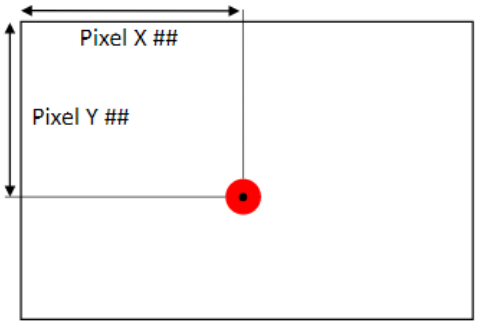

Figure 3. Representative image of the boresight alignment measurement.

1.2.2 Average Spot Size Measurement

To perform the spot size test, a collimating lens, ground glass diffuser, and fixed frequency glass grid were placed in between the laser source and optics. The detector captured an image with grid spots, as depicted in Figure 5, after which the average spot size was determined using an image processing software algorithm. Changes in image clarity were quantified by this measurement.

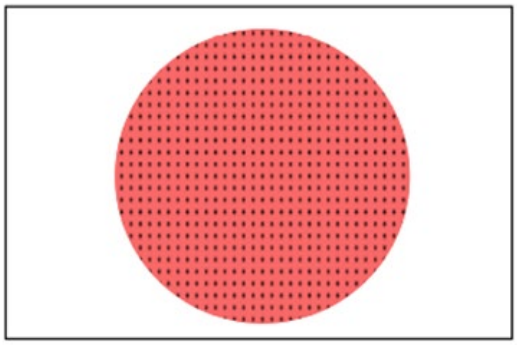

Figure 4. Representative image of the spot size measurement.

1.2.3 Field of View Measurement

The two side mirrors were configured coplanar with respect to each other, and they were perpendicular to the light path. The rotary stage was used to rotate the laser until it was offset 15° from the light path. The measurement was repeated in the other direction to account for the entire 30° field of view. An illustration of the FOV measurement is depicted in Figure 4. The FOV measurement was only taken twice – once before the environmental tests and once afterward.

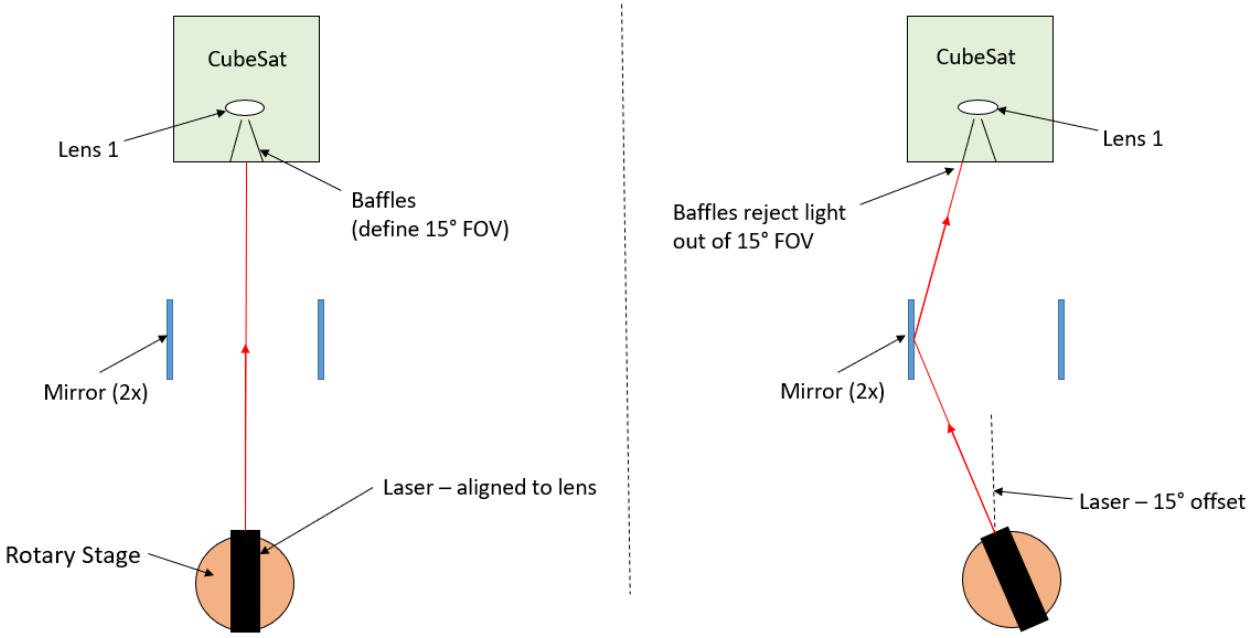

Figure 5. Illustration of the Field of View measureme/nt.

1.3 Environmental Conditions

1.3.1 Thermal Vacuum Specifications

The testing scope for this development was characterized as mechanical workmanship on a component level of assembly. The component level testing in section 2.6 of GEVS requires eight thermal cycles with a four-hour dwell per cycle. However, this TVAC test was purposed for static mechanical hardware, so as little as two cycles were sufficient for survivability demonstration. Furthermore, the assembly was small and built from aluminum, which means the hardware would quickly reach thermal equilibrium. Therefore, the TVAC test consisted of two thermal cycles with a two-hour dwell time per cycle. The temperature targets were set at 0 °C and 40 °C. The pressure inside the chamber was regulated to around 1E-5 Torr during the test.

1.3.2 Random Vibration Specifications

The vibration specifications were determined by NASA GEVS for prototype qualification standards [1]. A low-level sine signature test was conducted at an acceleration spectral density level (ASD) of 0.1 g, and the frequency ranged from 5 to 2000 Hz. The full level random vibration profile can be seen in Figure 6 below.

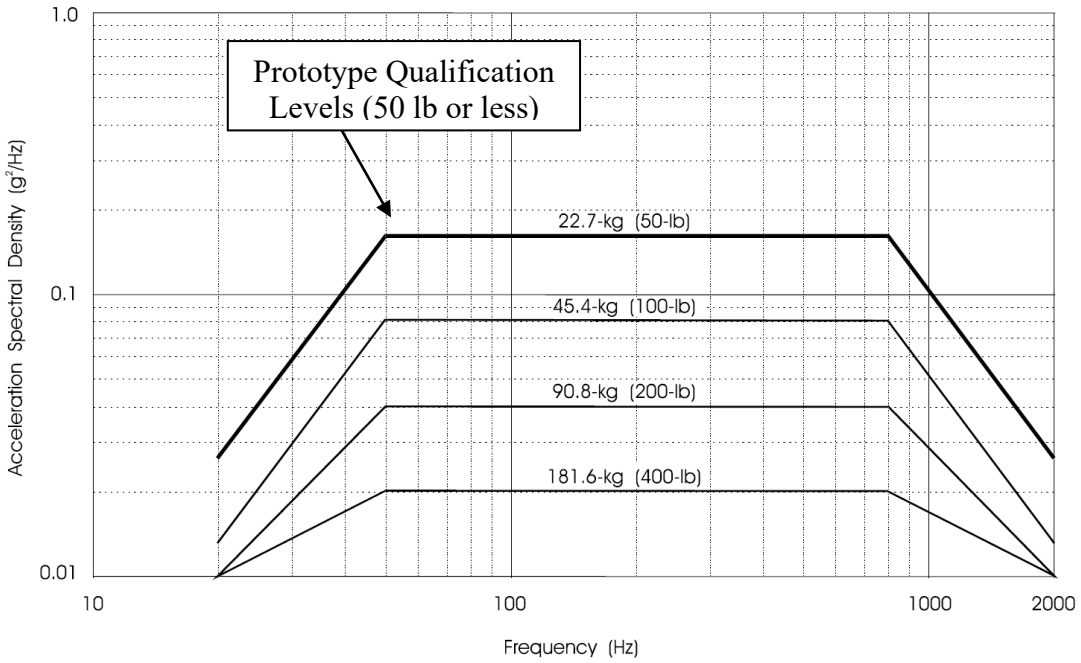

Figure 6. NASA GEVS specification for random vibration levels [1].

1.4 Experimentation Goals and Desired Results

The goal of the Cal Poly team was to successfully demonstrate the survivability of the instrument to launch environments. Cal Poly subjected the instrument to thermal vacuum and vibration environments, and collected image performance measurements before and after each test. The desired outcome of the testing was to establish the instrument maintained its optical alignment post-flight with respect to its initial on-ground alignment. Repeatability of the image measurements was determined to characterize the reliability of the image performance results.

2. EXPERIMENTATION

2.1 Imaging Support Equipment

An Atik 11000 series monochromatic Charge-Coupled Device (CCD) camera was used to capture visible light images from the instrument. This camera was selected for its high-resolution sensor. Each pixel was 9 µm x 9 µm with a horizontal and vertical resolution of 4007 pixels and 2671 pixels, respectively. Figure 7 shows the orientation of the CCD behind the instrument.

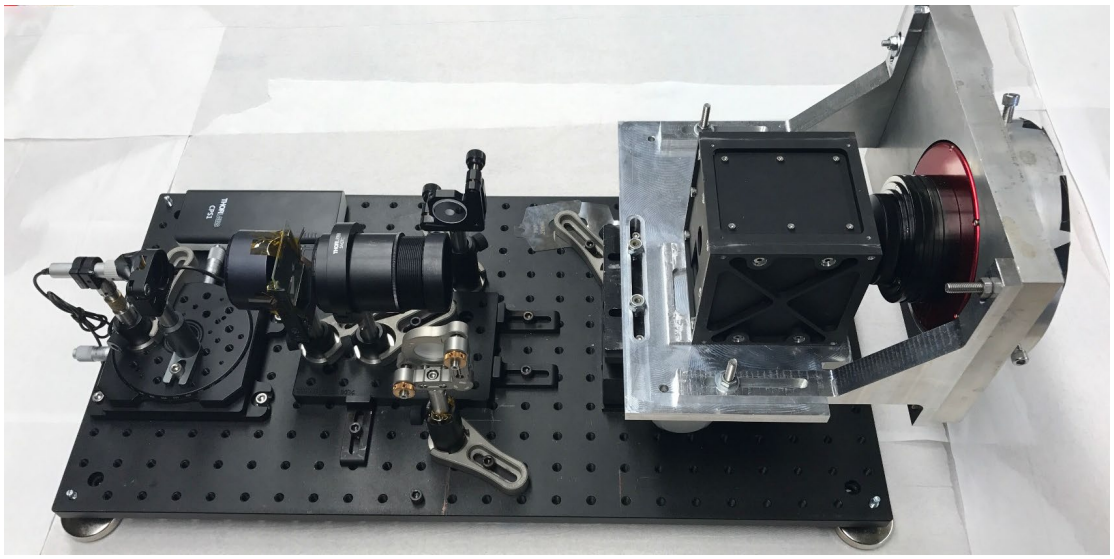

Figure 7. OGSE setup with the monochromatic CCD behind the instrument.

The OGSE was covered with a dark blanket to reduce stray light sources when taking the images. The research team took this precaution to improve the quality of the images, since the CCD was extremely sensitive to out of field stray light. Figure 8 shows an example of the images taken for each measurement.

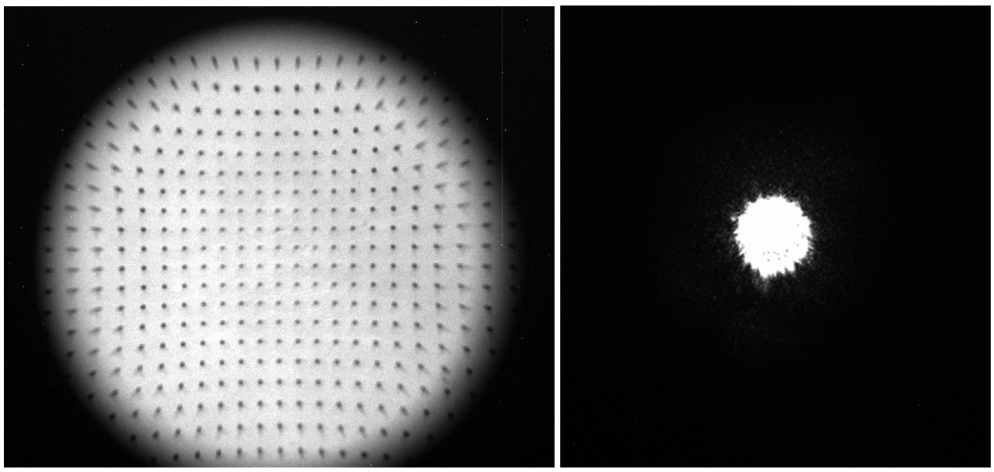

Figure 8. Demonstration of the spot size (left) and boresight (right) images.

2.2 TVAC Environment Test

2.2.1 TVAC Configuration

The thermal vacuum test was performed in the Aerospace Engineering hangar at Cal Poly's CubeSat facility. Two copper shrouds provided heating and cooling to the instrument, which was resting on the bottom shroud. Thermocouples were installed on the top shroud, bottom shroud, instrument structure, and instrument optics mount to record the temperatures during the test. The TVAC configuration is shown in Figure 9.

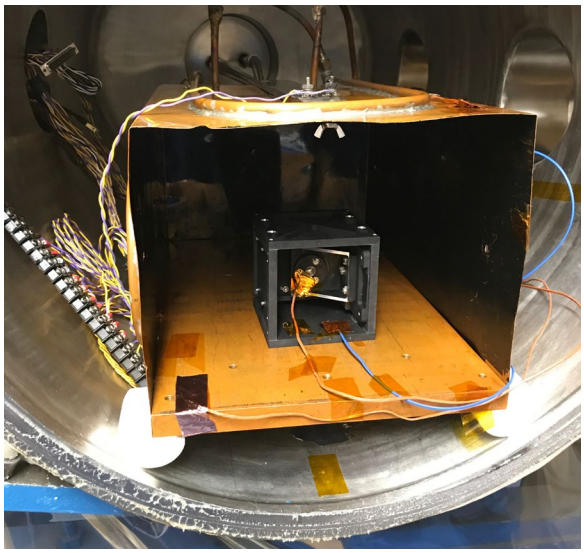

Figure 9. Instrument inside the TVAC chamber with thermocouples installed.

2.2.2 TVAC Environment Data

The temperature profile for the TVAC test is presented in Table 2. There were inaccuracies in the recorded temperature profile because the temperature of the shrouds was manually controlled. Furthermore, the liquid nitrogen supply tank was reconfigured in between the third and fourth cycle. Despite these discontinuities, the TVAC test was still valid because the instrument experienced all four thermal soaks for the required dwell time.

Table 2. Temperature profile including four thermal cycles.

Cycle	Temperature (°C)	Dwell Time (hr)
1	40	2
2	0	2
3	40	2
4	0	2

2.3 Vibration Environment Test

2.3.1 Vibration Configuration

The vibration tests were performed in the Mechanical Engineering vibrations laboratory at Cal Poly. Accelerometers were placed on the shake table, 1U deployer mount, instrument structure, and instrument optics mount. A 1U deployer was used to replicate the boundary conditions of a typical CubeSat deployer, but the deployer mount did not have an orbit-insertion mechanism behind the instrument. Thus, some of the dynamics associated with the compressed deployment spring were not captured in these tests. The vibration configuration is shown in Figure 11.

Figure 10. Instrument inside the 1U deployer shake table mount (left) and shake table setup with accelerometers installed (right).

2.3.2 Vibration Environment Data

The research team collected acceleration data from the four channels described above. The vibration data for the three axes is presented in Figure 12 through Figure 17. The sequence of operations for the three vibration tests is described below.

1. Install accelerometers at prescribed locations with sensor mounting wax and route cables
2. Secure instrument inside 1U deployer mount and install the cover plate
3. Torque the deployer mount fasteners and strain relieve the cables to the shake table
4. Run the first Low-Level Sine-Signature Test and verify response to expected results
5. Run the Random Profile Test in the following order: -12 dB, -6 dB, 0 dB and verify
6. Run the second Low-Level Sine-Signature Test and verify response
7. Take image performance measurements (boresight and spot size)

The instrument was tested in three cartesian axes, with each axis following the same sequence. First, a low-level sine-signature sweep was recorded to detect the natural frequency modes. Second, three random excitation profiles were used to subject the instrument to simulated flight vibration. Afterwards, a low-level sine-signature was recorded and compared to the first sine-signature to observe any peak shifts. The bode plots for the low-level sine (LLS) and random excitation tests are shown in sections 2.3.2.1-2.3.2.3 below. Note, the natural frequency of the instrument was found to shift slightly to the left in all three axes after undergoing random vibration excitation. This is an indication of component settling during the full-level random input. Furthermore, dynamic coupling is observed in all of the responses past 1000 Hz.

2.3.2.1 Axis 1

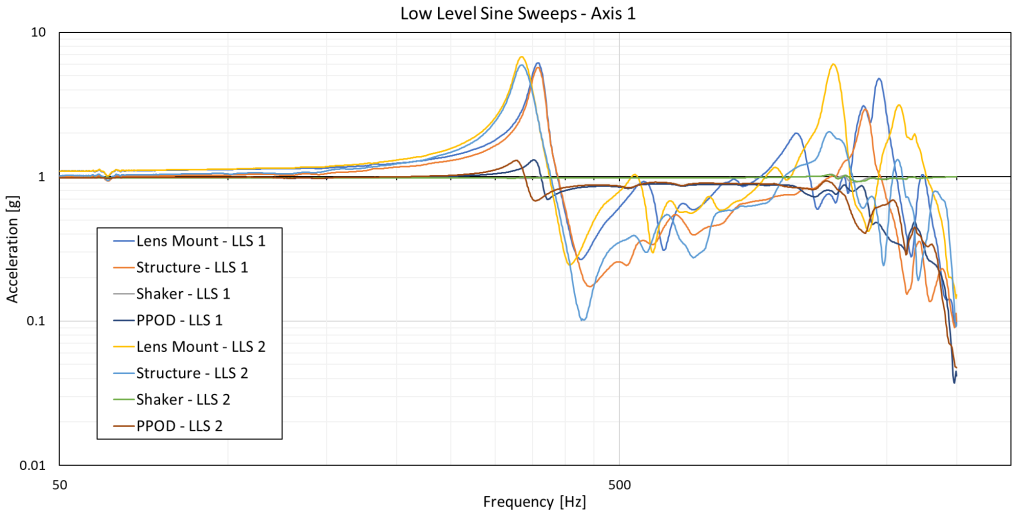

Figure 11. Low-level sine-signature sweeps for axis 1 of the instrument.

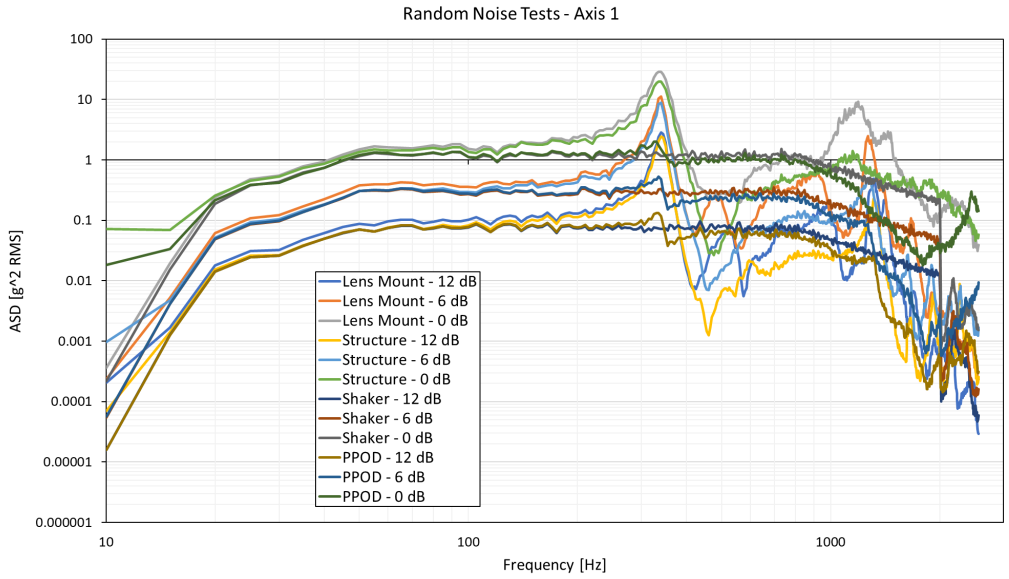

Figure 12. Random excitation response for axis 1 of the instrument.

2.3.2.2 Axis 2

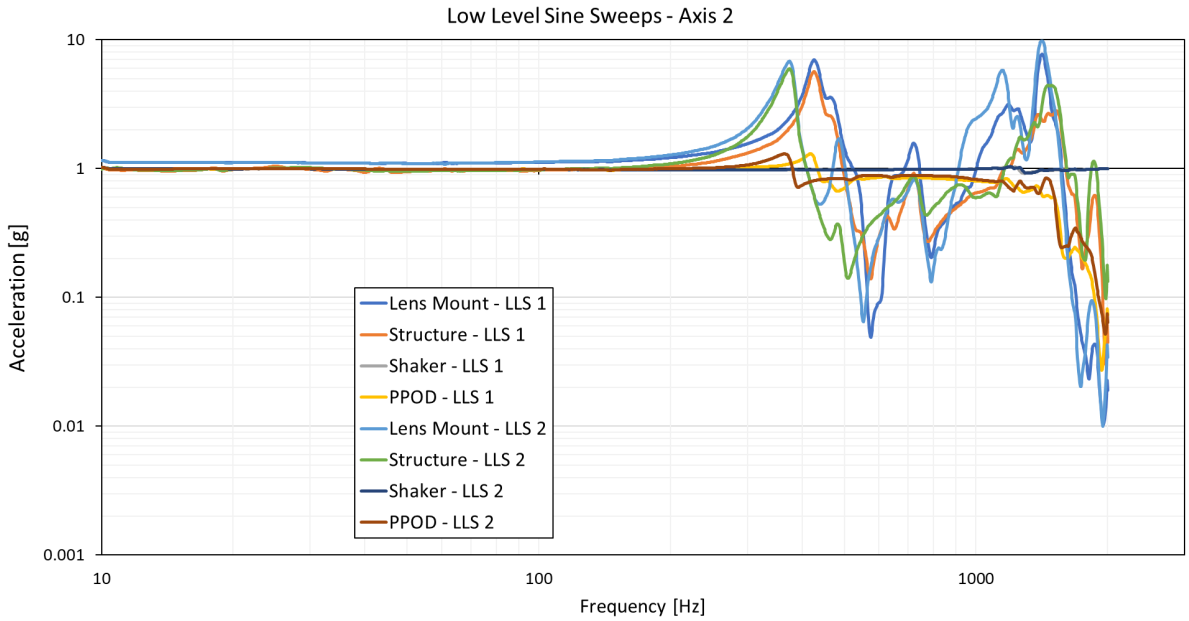

Figure 13. Low-level sine-signature sweeps for axis 2 of the instrument.

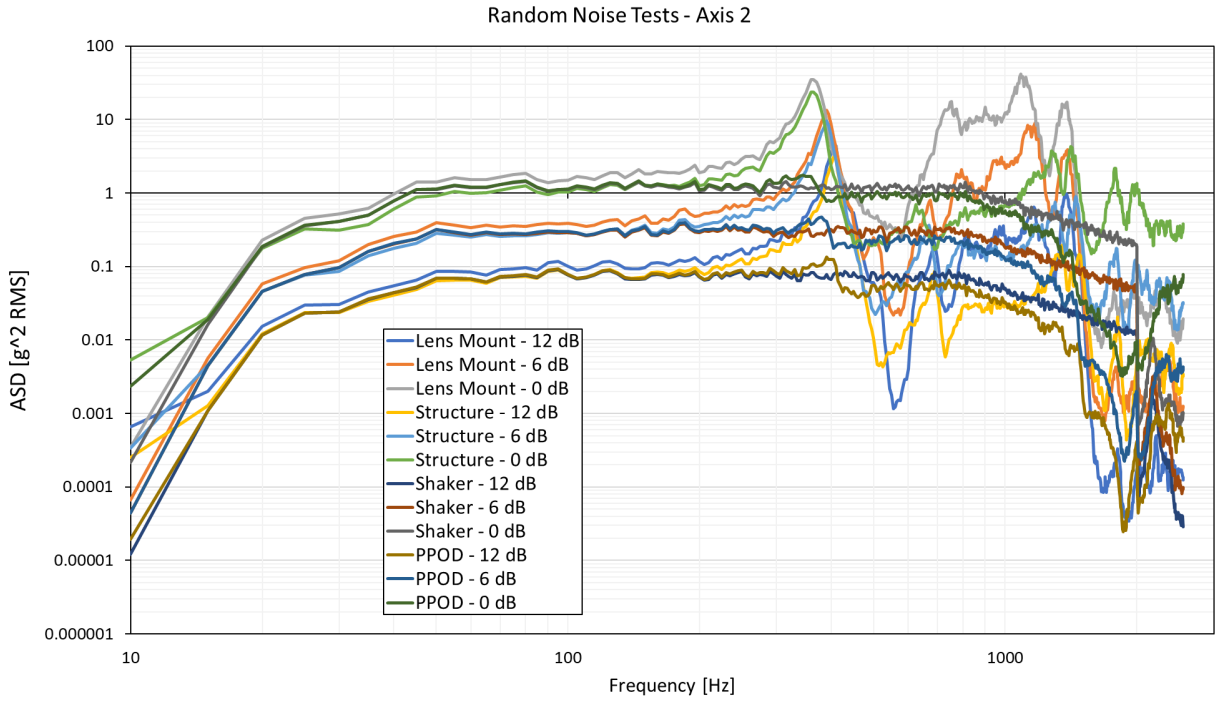

Figure 14. Random excitation response for axis 2 of the instrument.

2.3.2.3 Axis 3

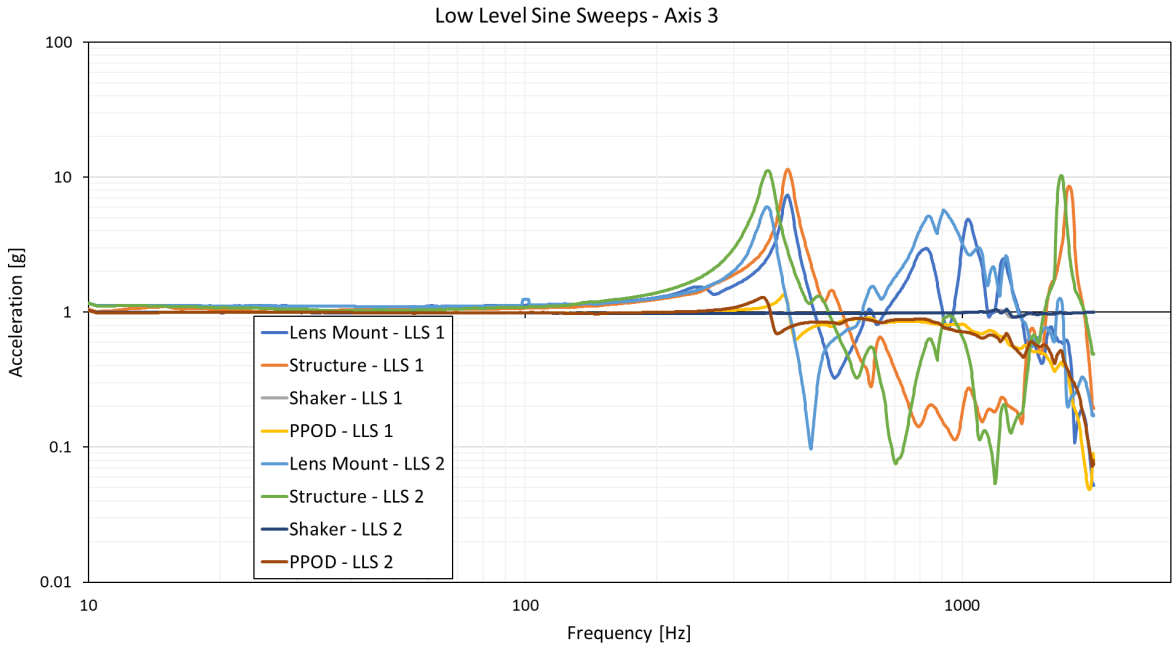

Figure 15. Low-level sine-signature sweeps for axis 3 of the instrument.

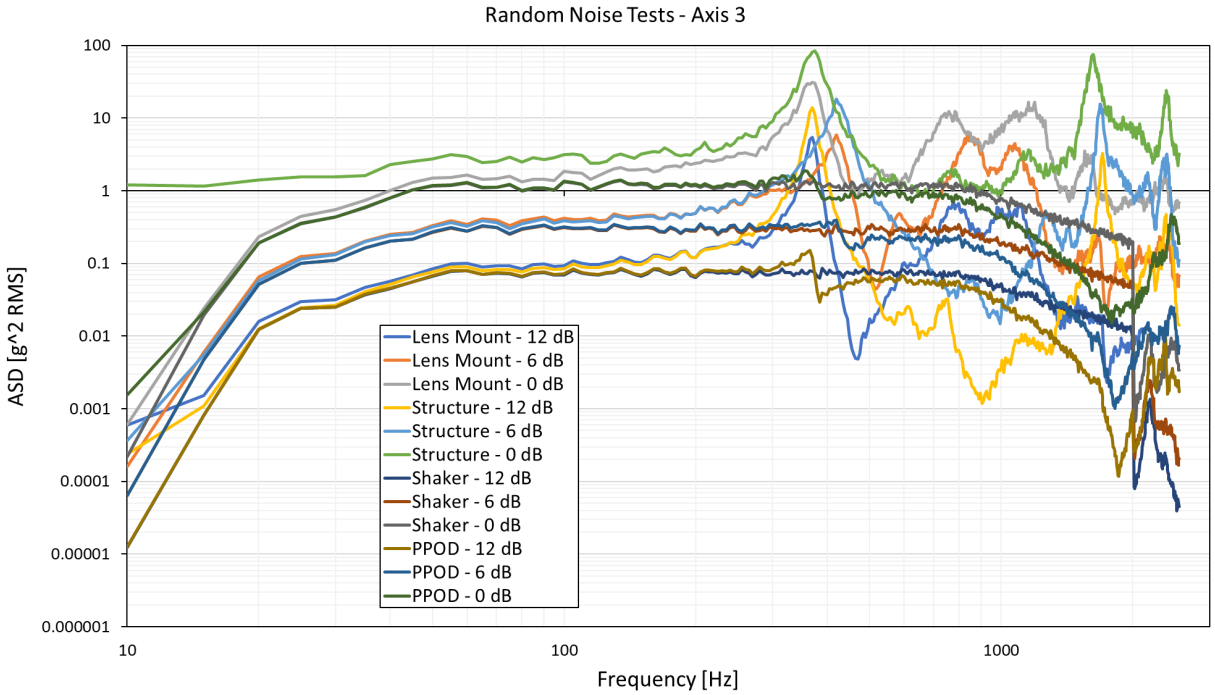

Figure 16. Random excitation response for axis 3 of the instrument.

3. RESULTS

3.1 Instrument Performance

Automated image processing was used to analyze the performance measurements. MATLAB's image processing toolbox provided a refined solution for this application. For the boresight measurement, a script was written to detect the average centroid location of the laser in pixels. An example of the script output for one of the boresight images is shown in Figure 18.

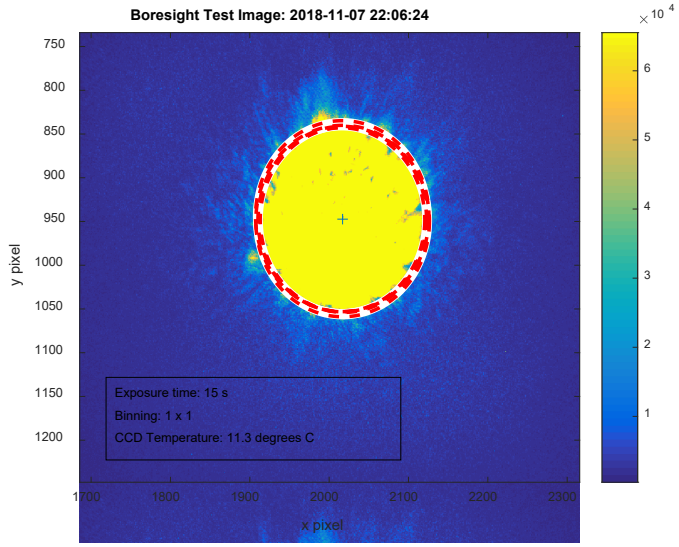

Figure 17. Example of the MATLAB algorithm output for the boresight measurement.

Similarly, another script was written to detect and count the size of individual spots in the spot size image. Based on the CCD pixel size of 9 µm x 9 µm, the diameter of each spot was calculated in microns. A histogram of the data was plotted and analyzed to find the average spot size. An example of the script output for one of the spot size images is shown in Figure 19.

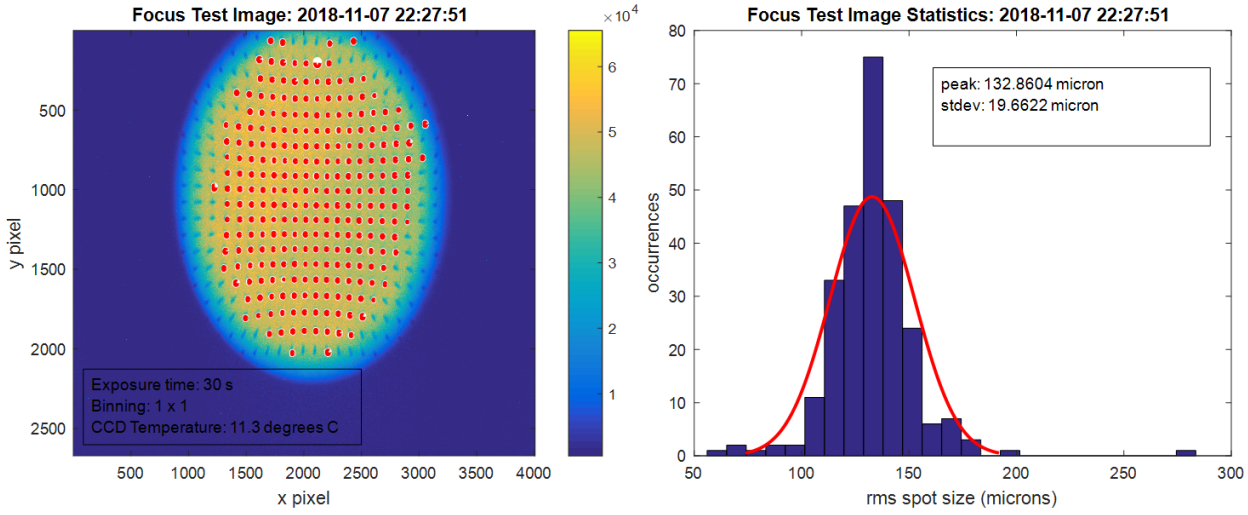

Figure 18. Example of the MATLAB algorithm output for the spot size measurement.

Although the complete array of instrument performance images is not included in this paper for brevity purposes, the summarized performance results are presented in Table 2. The uncertainty of each measurement was calculated at a 95% confidence interval; see Section 3.2 for more details regarding the measurement repeatability calculations.

Table 3. Image performance results for the instrument throughout the environmental tests.

Performance Test	**Boresight Alignment [x, y pixels]**	**Spot Size [µm]**	**Field of View [°]**
Pre-TVAC	[2017.4, 947.4]	132.86; σ = 19.66	29.6
Post-TVAC	[2017.3, 948.0]	133.26; σ = 19.26	-
Post-Vibe Axis 1	[2017.4, 947.2]	135.04; σ = 24.27	-
Post-Vibe Axis 2	[2016.7, 948.6]	132.03; σ = 20.63	-
Post-Vibe Axis 3	[2017.5, 947.6]	134.07; σ = 21.58	30.0
Uncertainty (95% Confidence)	± [0.9, 1.1]	± 5.06	± 0.8

For a visual representation of the boresight alignment throughout the course of environmental testing, reference Figure 20. Tight grouping of the centroid location is observed for all of the environmental tests, except for a slight shift to the left after the Axis 2 vibration test. This can be attributed because the excitation direction during the Axis 2 test was orthogonal to the optics boresight. Even though there is some deviation in boresight, the alignment maintenance requirement of 0.25° translates into an allowable deviaition of 22.3 pixels from the Pre-TVAC measurement. It is clear that the maximum deviation is about 1 pixel, or 0.011°, which is an order of magnitude below the design specification.

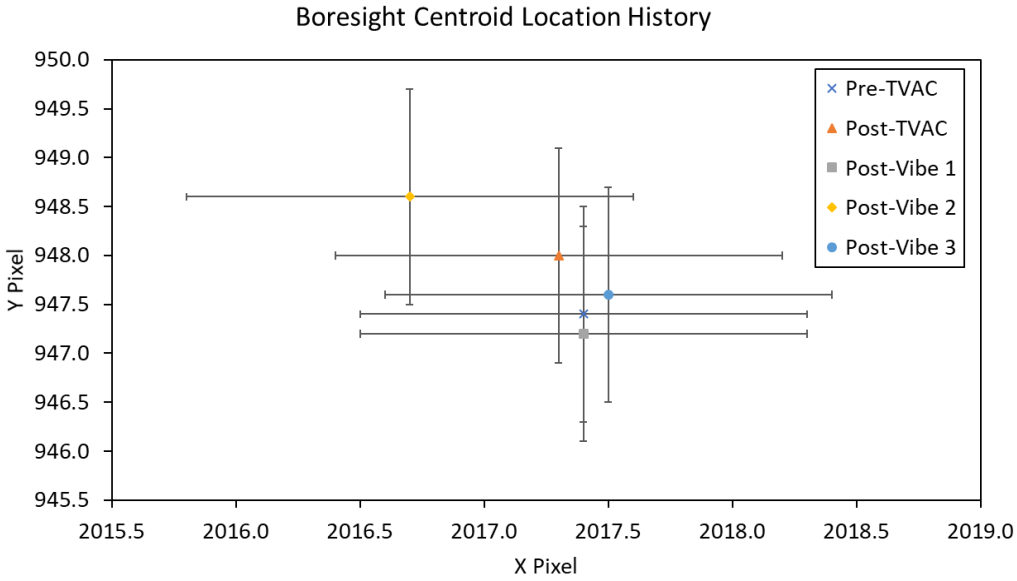

Figure 19. Graphical representation of the boresight alignment results.

Likewise, a visual representation of the spot size measurement throughout the course of the environmental testing is shown in Figure 21. On a high level, the spot size image is an indirect measurement of the relative distance between the two lenses. If the distance between the lenses change, the different focal length alters the size of the grid spots. It was observed that after the Axis 1 vibration test, where the excitation direction was in line with the two lenses (worst case scenario), the average spot size increased about two microns compared to the Pre-TVAC reference. This is an acceptable deviation, because the design specifies an allowable average spot size deviation of 20 microns. In like manner to the instrument boresight, the instrument's spot size performance was an order of magnitude below the design requirement.

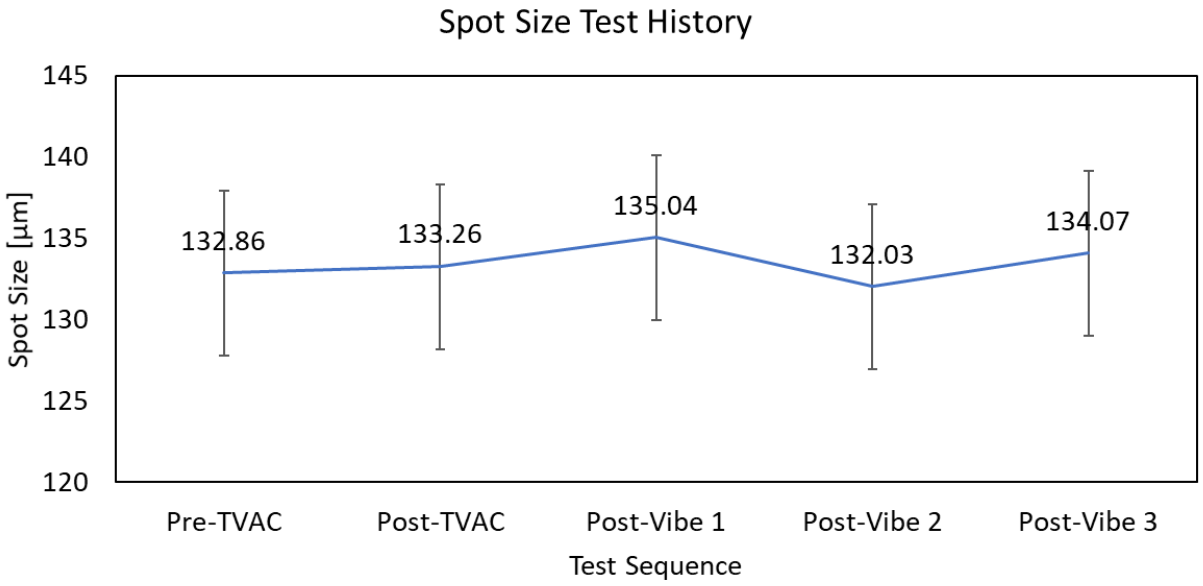

Figure 20. Graphical representation of the spot size results.

3.2 Measurement Repeatability

Data is only useful if one knows its accuracy. To calculate the uncertainty in the image performance measurements, a series of repeatability measurements were taken. The boresight measurement was taken 5 separate times after the instrument was removed and replaced onto the OGSE baseplate. The results are shown in Table 3.

Table 4. Repeatability of the boresight alignment measurements.

BORESIGHT		
Trial	**X [pixel]**	**Y [pixel]**
1	2020.5	954.9
2	2020.4	955.4
3	2020.8	955.6
4	2020.3	955.2
5	2021.0	955.8
Mean	2020.6	955.4
Std. Dev.	0.29	0.35
95% Confidence	**0.9**	**1.1**

In similar fashion, the spot size measurement was taken 5 separate times after the instrument was removed and replaced onto the OGSE baseplate. The results are shown in Table 4.

Table 5. Repeatability of the spot size measurements.

SPOT SIZE			
Trial	**Average Spot Size [µm]**	**Std. Dev. [µm]**	**Num. Spots**
1	132.62	20.93	268
2	132.36	21.57	298
3	130.57	20.95	251
4	131.00	19.56	262
5	134.80	18.56	275
Mean	132.27	20.38	
Std. Dev.	1.66	-	
95% Confidence	**5.06**		

And finally, the 0.8° uncertainty in the Field of View (FOV) measurement was calculated using the method of uncertainty propagation. This calculation consisted of the uncertainty in the mirror placement and the resolution of the laser rotation stage.

4. CONCLUSIONS

Vibration and thermal vacuum environmental tests were performed on the front 1U optics assembly of an ultraviolet imaging cube satellite. The instrument's image performance was measured in three manners using Optical Ground Support Equipment. First, the instrument FOV was measured to be 29.6° ± 0.8°. Second, the instrument boresight was measured to be [2017.4, 947.4] pixels, as captured by the CCD. And third, the average spot size was measured to be 132.9 microns. The instrument was then subjected to a thermal vacuum environment and a three-axis vibration environment to simulate the conditions experienced during launch and orbit. After each environmental test, the instrument's boresight and spot size was measured and observed to remain an order of magnitude below the allowable deviation defined by the design requirements. To validate the boresight and spot size image measurements, repeatability tests were conducted to establish the uncertainty in the measurements at a 95% confidence interval.

It was observed in the vibration data that the low-level sine-signature frequency response of the instrument shifted slightly to the left after the instrument was subjected to the random vibration. The reason for the shift is thought to be caused by component settling during the full vibe level. Furthermore, the natural frequencies of the shake table and deployer mount were both around 1500 Hz, which led to dynamic coupling when the system was subjected to the full random input. The instrument performance data shows exceptional margin despite the harsh vibration environment. Therefore, the instrument boresight alignment will remain within 0.25° and the spot size will be within 20 µm with respect to its initial on-ground alignment.

5. REFERENCES

1. NASA GODDARD SPACE FLIGHT CENTER. *General Environmental Verification Standard (GEVS)*. Greenbelt, Maryland: NASA, 2013. Print.
2. J. Grillo, T. Hajjar, B. Hill, E. Elghandour, K.Rider, T.J. Immel. *Characterizing Multifunctional Materials to Mitigate Vibrations Induced on Spacecraft Optical Equipment*. Dallas, Texas: CAMX, 2018.
3. J. Grillo, T. Hajjar, B. Hill, E. Elghandour, K.Rider, T.J. Immel. *Ultraviolet Imager Application for a Cube Satellite*. Cal Poly San Luis Obispo, 2018.
4. P.B. Hays, T.L. Killeen, N.W. Spencer, L.E. Wharton, R.G. Roble, B.A. Emery, T.J. Fuller-Rowell, D. Rees, L.A. Frank, J.D. Craven. *Observations of the Dynamics of the Polar Thermosphere*. J. Geophys. Res. 89, 5597–5612, 1984.
5. J.P. Thayer, T.L. Killeen, F.G. McCormac, C.R. Tschan, J.-J. Ponthieu, N.W. Spencer. *Thermospheric Neutral Wind Signatures Dependent on the East-West Component of the Interplanetary Magnetic Field for Northern and Southern Hemispheres as Measured from Dynamics Explorer-2*. 5A(6), 363–368, 1987.
6. T.J. Immel, J.C. Foster, A.J. Coster, S.B. Mende, H.U. Frey. *Global Storm Time Plasma Redistribution Imaged from the Ground and Space*. Geophys. Res. Lett. 32, 3107, 2005.
7. T.J. Immel, E. Sagawa, S.L. England, S.B. Henderson, M.E. Hagan, S.B. Mende, H.U. Frey, C.M. Swenson, L.J. Paxton. *The Control of Equatorial Ionospheric Morphology by Atmospheric Tides*. Geophys. Res. Lett. 33, 15108, 2006.